ARTICLES
PUBLISHED ONLINE: 26 OCTOBER 2015 | DOI: 10.1038/NCLIMATE2830
nature climate change

Old soil carbon losses increase with ecosystem respiration in experimentally thawed tundra

Caitlin E. Hicks Pries*†, Edward A. G. Schuur†, Susan M. Natali† and K. Grace Crummer

Old soil carbon (C) respired to the atmosphere as a result of permafrost thaw has the potential to become a large positive feedback to climate change. As permafrost thaws, quantifying old soil contributions to ecosystem respiration (R_{eco}) and understanding how these contributions change with warming is necessary to estimate the size of this positive feedback. We used naturally occurring C isotopes ($\delta^{13}C$ and $\Delta^{14}C$) to partition R_{eco} into plant, young soil and old soil sources in a subarctic air and soil warming experiment over three years. We found that old soil contributions to R_{eco} increased with soil temperature and R_{eco} flux. However, the increase in the soil warming treatment was smaller than expected because experimentally warming the soils increased plant contributions to R_{eco} by 30%. On the basis of these data, an increase in mean annual temperature from −5 to 0 °C will increase old soil C losses from moist acidic tundra by 35–55 g C m^{-2} during the growing season. The largest losses will probably occur where the plant response to warming is minimal.

Soils and sediments in the northern circumpolar permafrost zone store two times the amount of C as is in our atmosphere (~1,672 Pg; ref. 1) because frozen soil conditions have protected organic C from decomposition for hundreds to thousands of years[2,3]. The temperature increases (5–9 °C) predicted for high northern latitudes over the next century[4] will make much of the world's permafrost vulnerable to thaw. Models predict that 6–29% of permafrost will be lost for each degree of warming[5]. Model simulations also indicate that permafrost thaw has already occurred due to active layer thickening at a rate of 10 cm per decade in some areas[6]; such thaw has been documented in Alaska[7], Greenland[8] and Siberia[9]. Concurrent with permafrost thaw is C loss as these previously frozen soils are exposed to increased microbial activity. To better predict the size of the permafrost C feedback, the vulnerability of old soil C to thaw and warming needs to be quantified[10].

Globally, respiration increases with greater mean annual temperatures[11]. Numerous warming experiments in permafrost ecosystems have found R_{eco} increases with warming[12–16]. Despite many studies on the response of R_{eco} to warming, it remains unclear how much of that response is due to increased microbial activity, which leads to losses of the critical old soil C pool. Both plant (autotrophic; R_A) and microbial (heterotrophic; R_H) respiration increase with warming[13,17,18]; thus old soil C contributions to R_{eco} cannot be quantified by measuring land–atmosphere fluxes alone[19,20].

Whether R_A or R_H drives the increase in R_{eco} determines whether or not a large positive feedback to climate change is occurring or has the potential to occur. Increased plant respiration is not a positive feedback to climate change because, on the timescales over which climate change is occurring, R_A is generally balanced by production, whereas R_H is not. This imbalance is extreme in permafrost ecosystems where soil C has been accumulating since the start of the Holocene epoch[2], or even during the Pleistocene, as in unglaciated regions of Siberia and Alaska[21]. The potential effect of increased R_H on atmospheric CO_2 levels is much greater than that of increased R_A because the soil C pool is orders of magnitude larger than the plant C pool in permafrost ecosystems.

Natural tracers partition R_{eco} into auto- and heterotrophic sources with minimal disturbance to the ecosystem. $\delta^{13}C$ or $\Delta^{14}C$ have often been used separately to estimate source contributions to respiration[14,22–24]. However, using both C isotopes is more powerful because it allows R_{eco} to be partitioned into more sources more accurately than with a single isotope[25]. Natural abundance $\delta^{13}C$ and $\Delta^{14}C$ separate sources based on different principles. $\delta^{13}C$ separates respiration sources by means of biological fractionation[26], and $\Delta^{14}C$ separates respiration sources by age—on millennial timescales as a result of radioactive decay, and on annual to decadal timescales using the bomb enrichment of atmospheric ^{14}C (ref. 24).

Here, we used natural abundance $\delta^{13}C$ and $\Delta^{14}C$ to partition R_{eco} at CiPEHR (Carbon in Permafrost Experimental Heating Research), a warming experiment in Alaskan subarctic tundra[15,27]. CiPEHR is unique among tundra warming experiments because it warms deep soil, causing permafrost thaw without confounding effects such as altered growing season length or water inputs. CiPEHR uses snow fences (with the excess snow removed each spring) to insulate soils during the winter (soil warming), which results in soils that are 1.5 °C warmer than the control during the growing season and increases thaw depths by 10% (ref. 15). Open-top chambers warm air in the summer (air warming) by about 1 °C, but do not affect soil temperatures[15]. After three years of experimental soil warming at CiPEHR, R_{eco} increased up to 57% relative to controls[15]. To investigate the contribution of old soil C loss to this R_{eco} increase, we partitioned R_{eco} into autotrophic (both aboveground and belowground plant structures), young surface soil (post-1963 bomb peak; 0–15 cm), and old deeper soil (15–75 cm) sources. This is the first study to present process-level relationships of how R_{eco} sources respond to soil temperature and experimental warming in a permafrost ecosystem.

Department of Biology, University of Florida, PO Box 118525, Gainesville, Florida 32611, USA. †Present addresses: Climate Sciences Department, Earth Sciences Division, 1 Cyclotron Rd, Lawrence Berkeley National Laboratory, Berkeley, California 94720, USA (C.E.H.P.); Center for Ecosystem Science and Society, Department of Biological Sciences, Northern Arizona University, Flagstaff, Arizona 86011, USA (E.A.G.S.); Woods Hole Research Center, 149 Woods Hole Road, Falmouth, Massachusetts 02540, USA (S.M.N.). *e-mail: cehpries@lbl.gov

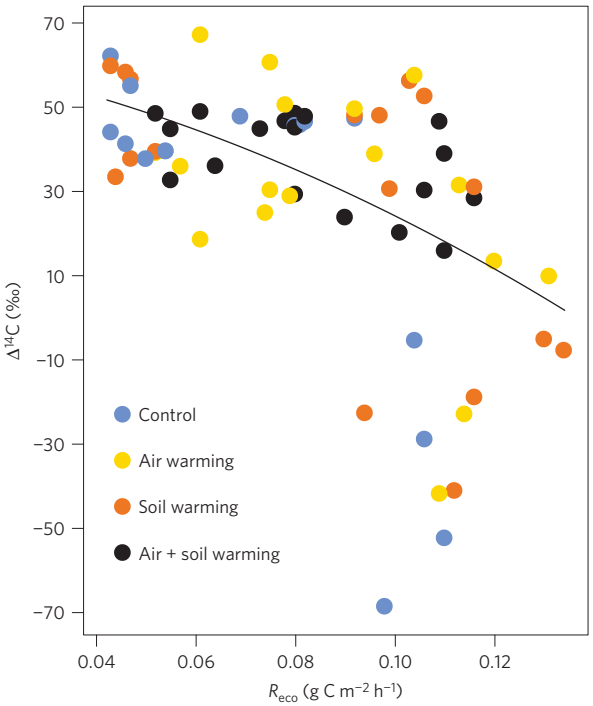

Figure 1 | $R_{eco}\Delta^{14}C$ decreased as ecosystem respiration fluxes increased. The points are the data and the solid line is the prediction of the linear regression (see Table 1).

Results and discussion

Ecosystem respiration $\Delta^{14}C$ became significantly more depleted with increases in R_{eco} (Fig. 1 and Table 1) and in depth-averaged soil temperature (hereafter called soil temperature; Fig. 2a and Table 1). The depletion in $\Delta^{14}C$ with increased temperature was more pronounced in the control than in the experimental warming treatments (Fig. 2a and Table 1). Ecosystem respiration $\Delta^{14}C$ was not affected by water table depth or soil moisture in our moist tundra; these variables were not significant predictors in the regression model. In contrast, wetting events caused a significant enrichment in soil $\Delta^{14}CO_2$ in semi-desert tundra[28].

More depleted $R_{eco}\Delta^{14}C$ with increased soil temperatures indicated that warming caused a shift in respiration sources. Ecosystem respiration $\Delta^{14}C$ has previously been shown to become more depleted[20] or more enriched[29] with permafrost thaw, which is positively correlated with soil temperature. Both $\Delta^{14}C$ shifts were due to increases in the contribution of heterotrophic sources to R_{eco}, although the age of the dominant heterotrophic sources differed in the two studies.

To understand which R_{eco} sources were driving the temperature-mediated depletion in $R_{eco}\Delta^{14}C$, we used a dual-isotope ($\delta^{13}C$ and $\Delta^{14}C$) mixing model to estimate proportional contributions of plant and soil respiration to R_{eco} (Supplementary Table 1). Respiration $\Delta^{14}C$ and $\delta^{13}C$ differed significantly among sources. Over all sampling dates, aboveground $R_A\Delta^{14}C$ averaged 42.1 ± 1‰ and roughly matched the value of the atmosphere in the year it was sampled. Belowground R_A (49.2 ± 2‰) was significantly more enriched than aboveground R_A, indicating belowground R_A was a few years older on average ($p = 0.007$; Supplementary Table 2). Belowground $R_A\delta^{13}C$ averaged -25.3 ± 0.2‰ and was always about 3‰ more depleted than aboveground R_A, which averaged -22.1 ± 0.2‰ ($p < 0.0001$; Supplementary Table 2). Surface soil (0–15 cm) $R_H\Delta^{14}C$ averaged 88 ± 2‰ (about ten years old) and was significantly more enriched in $\Delta^{14}C$ than deeper soil (15–75 cm) R_H, which averaged -82 ± 8‰ ($p < 0.0001$; Supplementary Table 3). Carbon emitted by deeper soil R_H was on average 665 years old, and the oldest respired C we measured was 6,000 years old. These ages represent the relative age of respired CO_2, but not exact years because respiration is probably a mixture of younger and some much older C. Surface soil $R_H\delta^{13}C$ averaged -23.6 ± 0.2‰ and was significantly more depleted in $\delta^{13}C$ than deeper soil R_H, which averaged -21.6 ± 0.2‰ ($p < 0.0001$; Supplementary Table 3).

The decrease in $R_{eco}\Delta^{14}C$ with soil temperature was caused by an increase in the proportion of respiration coming from the old soil C pool because the contribution of old soil to R_{eco} also increased significantly with soil temperature (Fig. 2b and Table 1). Rising temperatures can cause more of the older C pool to become available to microbes in several ways. First, deeper thaw increases the size of the old C pool available to above-freezing decomposition. Second, older C may be more chemically recalcitrant than younger C, so that its decomposition requires higher activation energies and is thus more sensitive to temperature[18]. Further evidence that old soil respiration was at least partially driving the R_{eco} increase was that old soil was a greater proportion of R_{eco} when flux rates were higher: for each 0.01 g C m^{-2} h^{-1} increase in R_{eco}, old soil contributed about 3% more to the flux (Fig. 3 and Supplementary Table 5). The overall range of old soil contributions to R_{eco} (3–73%) was slightly larger in this study than in previous studies from northern peatlands[14,30] and tundra[20,22], where the maximum old soil contribution was 45% (ref. 22).

The greatest contributions of old soil C to R_{eco} occurred during a time period when conditions for heterotrophic decomposition were optimal. Both old soil contributions and R_{eco} flux were greatest in August 2010, when mean R_{eco} was 0.10 g C m^{-2} h^{-1} versus 0.08 and 0.05 g C m^{-2} h^{-1} for August 2011 and 2009, respectively. August 2010 had the deepest thaw, the warmest soils, and the greatest soil moisture[31] of all sampling dates. These observations from a stochastically warm month of our three-year study add to our experimental evidence that environmental conditions that favour greater R_{eco} rates also increase contributions of old soil C.

The soil temperature responses of $R_{eco}\Delta^{14}C$ and old soil contributions to R_{eco} were affected by treatment (Fig. 2 and Table 1). In contrast to expectations, old soil contributed proportionally more to R_{eco} in the control than in the warming treatments. Smaller old soil proportional contributions in the warming treatments were caused by increased contributions from plant respiration. Both air and soil warming treatments had larger autotrophic contributions to R_{eco} (51–57%) than the control (44%), with the soil warming effect being significant (Table 1). Included in the autotrophic contributions is microbial respiration of fresh plant material such as root exudates. This type of microbial respiration is intimately dependent on plant production and releases C from the same fast cycling pool; thus it should respond to warming in a similar manner to that of autotrophs.

Plant respiration increased as a result of the soil warming treatment owing, in part, to increased aboveground net primary production[15], especially of graminoids, whose biomass increased in the soil warming treatments[15,32]. Increased plant productivity and biomass necessitated an increase in growth and maintenance respiration within the warming treatments[13,33]. The cause of the plant respiration increase was probably not a direct result of soil temperature or a release from water limitation (the soil warming treatments were wetter[15]) because temperature and soil water content were not significant predictors of autotrophic contributions in the regression model. Instead, it is likely that plants in the soil warming treatments responded to increased nitrogen availability because productivity is limited by nitrogen in the tundra[34,35]. Canopy nitrogen was greatest in soil warming plots[32], and nitrogen mineralization often increases with experimental warming or permafrost thaw[35,36].

The increase in old soil contributions with R_{eco} flux was greatest in the control and least in the soil warming treatments (Fig. 3

Table 1 | Significant predictors from stepwise linear regressions involving the depth-averaged soil temperature (ST), soil volumetric water content, thaw depth, water table depth and treatment ($n = 69$).

Response	Coefficients	Estimate	SE	*t* value	*p* value
$R_{eco}\Delta^{14}C$ (‰, reflected square root)	Intercept	−2.18	0.76	−2.90	<0.0051***
	R_{eco} flux	−44.49	8.7	−5.10	<0.00001***
$R_{eco}\Delta^{14}C$ (‰, reflected square root)	Intercept	2.72	2.10	1.29	0.2012
	Air warming	−5.89	2.55	−2.31	0.0240
	Soil warming	−4.47	2.52	−1.77	0.0811*
	Air + soil	−6.35	2.17	−2.92	0.0048**
	ST	−1.84	0.44	−4.16	0.0001***
	ST:Air	−0.51	0.30	−1.71	0.0922*
	ST:Soil	−0.79	0.28	−2.83	0.0063**
	ST:Air + soil	−0.35	0.10	−3.56	0.0006***
Old soil (proportion, logit)	Intercept	−4.56	0.96	−4.72	<0.00001***
	Air warming	1.52	1.17	1.30	0.198
	Soil warming	0.72	1.15	0.63	0.530
	Air + soil	2.38	1.13	2.10	0.0394**
	ST	0.68	0.19	3.51	0.0009***
	ST:Air	−0.39	0.23	−1.71	0.0928*
	ST:Soil	−0.28	0.22	−1.27	0.210
	ST:Air + soil	−0.59	0.22	−2.66	0.010**
Autotrophic (proportion, logit)	Intercept	−0.26	0.15	−1.8	0.085*
	Air warming	0.32	0.21	1.5	0.136
	Soil warming	0.56	0.21	2.7	0.010**
	Air + soil	0.29	0.21	1.4	0.171
R_A:R_H (log)	Intercept	−0.26	0.13	−1.9	0.05921*
	Air warming	0.32	0.19	1.6	0.10127
	Soil warming	0.57	0.19	2.9	0.00464**
	Air + soil	0.49	0.19	2.6	0.01144**

An additional regression was run for $R_{eco}\Delta^{14}C$ using just R_{eco} flux and treatment as predictors ($n = 69$). The units of and transformation used for the response variables are in parentheses. The coefficients reported here were not back transformed. The number of asterisks (*) indicates level of significance.

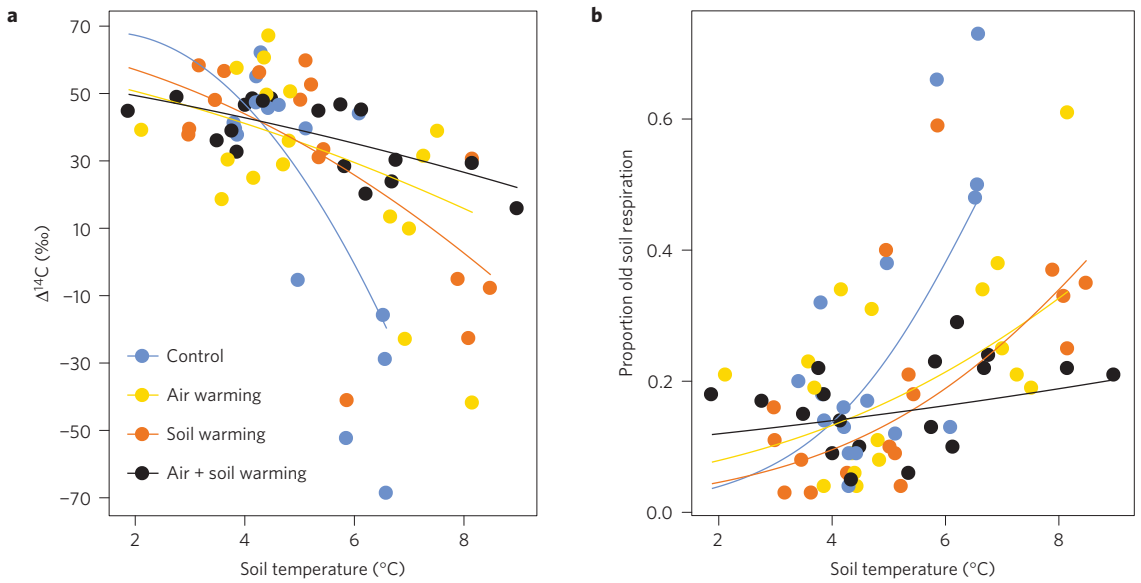

Figure 2 | Relationships with soil temperature. a,**b**, $R_{eco}\Delta^{14}C$ decreased (**a**) and old soil contribution to R_{eco} generally increased (**b**) with depth-integrated soil temperature. Experimental treatment changed the slope of these relationships (see Table 1 for model coefficients). Source partitioning indicated the $R_{eco}\Delta^{14}C$ relationship was driven by an increase in R_H from old, deeper soils (15–75 cm) that was partially masked by increased R_A in the warming treatments. The points are the data and the solid lines are the prediction of a linear regression.

and Supplementary Table 5). The increase was greatest despite the control having a shallower active layer[15] —and subsequently smaller volume of unfrozen old soil available for decomposition— and is not explained by soil moisture or water table, which had no significant effects in any regression. Although greater autotrophic contributions to R_{eco} relative to old soil contributions partially explain why old soil contributions are less responsive in the experimental warming treatments, increased autotrophic activity may decrease old soil C losses in other ways. Increased primary productivity in the warming treatments could reduce

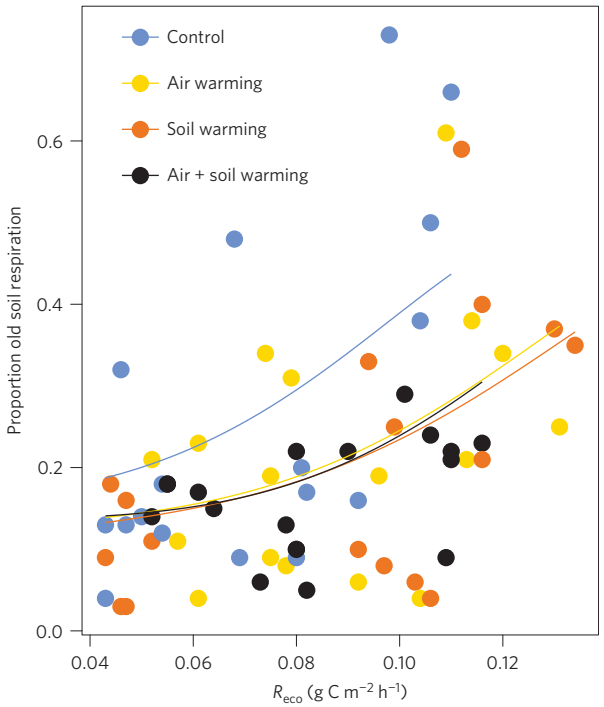

Figure 3 | Old soil contribution to R_{eco} increased with increasing respiration flux. This relationship changed significantly with treatment. The points are the data and the solid lines are the prediction of a linear regression (see Supplementary Table 5).

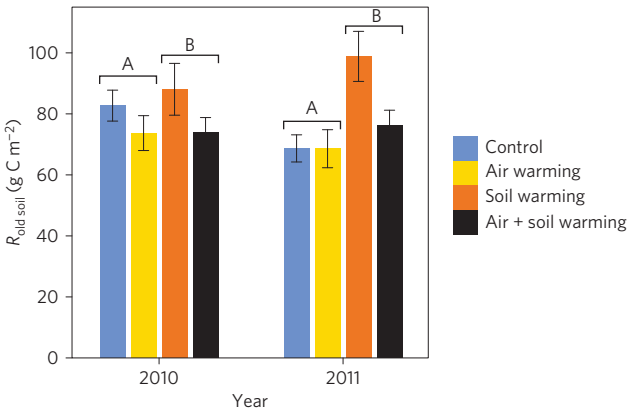

Figure 4 | Estimated growing season old C losses from the experimental treatments in 2010 and 2011. Old soil C losses are significantly greater in the plots with the soil warming treatment than in soil warming control plots ($p = 0.015$; indicated with letters not shared).

mineralization of old soil C owing to microbial preference for newer plant-derived substrates[37].

Despite the greater proportional contributions of old soil C to R_{eco} in the control plots, growing season C losses from old soil respiration were significantly greater in the soil warming treatments than in the soil warming control ($p = 0.0157$; Fig. 4). The control had smaller R_{eco} fluxes overall[15] (Fig. 3), leading to less old soil C loss, particularly in 2011. In 2010, only 6.5% more old soil C was released in the soil warming treatments as compared to the control, whereas in 2011, 44% more old soil C was released—a 30 g m^{-2} increase in C lost to the atmosphere during the growing season. Therefore, experimentally warming tundra and degrading the surface permafrost caused old soil C to be lost to the atmosphere.

However, air warming caused significantly less growing season old soil C loss than the air warming control ($p = 0.0102$; Fig. 4). Air warming lost 8.9 g C m^{-2} less than the control in 2010 and lost the same amount of old soil C as the control in 2011, in part because the air + soil warming treatment had the lowest proportional contributions from old soil when soil temperatures were warmest (Fig. 2b). Contrary to expectations, old soil C losses from the control were generally not much less than from the air or soil warming treatments, with the exception of the soil warming treatment in 2011.

Although other studies have demonstrated increased old soil C losses from permafrost ecosystems due to thaw or warmer temperatures[14,20], ours is the first to show how experimental treatments affect that relationship. The soil warming treatment caused a shift in the growing season C cycle from more heterotrophic to more autotrophic control of R_{eco}. Thus, the proportion of old soil contributions actually increases less in response to soil temperature in the soil warming than in the control treatments.

The relationship between R_{eco} and old soil proportional contributions can be used to estimate how losses of old soil C from tundra ecosystems change with warming temperatures, with the treatments' different responses reflecting a range of potential C losses. The responses of R_A and R_H to warming at this experiment were similar to those in a Swedish peatland[38]. Furthermore, amplification of the C cycle (greater R_{eco} and primary production) due to warming has been observed across many tundra ecosystems, including our site[39]. Tundra growing season R_{eco} increases about 13.3 g C m^{-2} for each 1 °C rise in mean annual temperature (MAT; ref. 39). Therefore, on the basis of our empirical relationship, an increase in MAT from −10 to −5 °C will cause the proportion of old soil contributions to R_{eco} to increase from 0.15–0.22 to 0.19–0.32, causing 19–35 g m^{-2} more old soil C loss each growing season. An increase from -5 to 0 °C will cause 35–55 g C m^{-2} more old soil C loss. The upper range of these estimates is from the empirical relationship of the control treatment data, which may be analogous to tundra ecosystems where the vegetation response to warming is limited. Thus, the growing season loss of old soil C due to warming depends in part on the autotrophic response, an interaction that warrants further study.

Implications for net ecosystem carbon balance

Overall, experimentally warming tundra caused an increase in R_{eco} that is driven by both plant and old soil respiration. The overall increase was driven more by autotrophs than heterotrophs, as demonstrated by the ratio of R_A to R_H, which is greater in the warming treatments than in the control (Table 1). The increase in autotrophic respiration is because plants are fixing more C as a result of the warming treatment such that the warming treatments are at present a growing season sink of 102 g C m^{-2} (ref. 15). This increase in plant productivity is masking the critical loss of old soil C that has the potential to become a long-term feedback to climate change. It is only by using isotopes that we have been able to detect and quantify this old soil C loss.

At present, the growing season loss of old soil C in the soil warming treatments is being compensated for by C taken up by increased plant growth and stored in biomass because the site is a growing season C sink[15]. However, because the soil C pool (60 kg m^{-2}; ref. 2) at our site is several orders of magnitude larger than the plant C pool (0.45–0.63 kg m^{-2}; ref. 32), old soil C losses have the potential to eventually surpass gains in plant biomass. Much depends on how future plant productivity will respond to rising temperatures, changing soil moisture, and increased atmospheric CO_2. One prediction for mesic tundra found that plant production would continue to outpace R_H for the next century[40]. However, at our experiment, the tipping point may have already been reached. This study examined only growing season R_{eco} dynamics, but soil warming increased winter R_{eco} by

50%, offsetting increased growing season C uptake[15]. Wintertime respiration increases are probably driven by old soil C losses because deep soils freeze last in the autumn, remain warmer than surface soils during the winter, and may form taliks (a layer of unfrozen soil between the permafrost and seasonally frozen soil)[22]. Old soil C losses due to warmer soils will probably continue into the winter and could lead to a positive climate change feedback even when the growing season C sink is increasing.

Methods

Methods and any associated references are available in the online version of the paper.

Received 18 August 2014; accepted 19 August 2015; published online 26 October 2015

References

1. Tarnocai, C. *et al*. Soil organic carbon pools in the northern circumpolar permafrost region. *Glob. Biogeochem. Cycles* **23**, GB2023 (2009).
2. Hicks Pries, C. E., Schuur, E. A. G. & Crummer, K. G. Holocene carbon stocks and carbon accumulation rates altered in soils undergoing permafrost thaw. *Ecosystems* **15**, 162–173 (2012).
3. Czimczik, C. & Welker, J. Radiocarbon content of CO_2 respired from high Arctic tundra in northwest Greenland. *Arct. Antarct. Alp. Res.* **42**, 342–350 (2010).
4. IPCC *Climate Change 2013: The Physical Science Basis* (eds Stocker, T. F. *et al*.) (Cambridge Univ. Press, 2013).
5. Koven, C. D., Riley, W. J. & Stern, A. Analysis of permafrost thermal dynamics and response to climate change in the CMIP5 Earth system models. *J. Clim.* **26**, 1877–1900 (2013).
6. Burke, E. J., Jones, C. D. & Koven, C. D. Estimating the permafrost-carbon climate response in the CMIP5 climate models using a simplified approach. *J. Clim.* **26**, 4897–4909 (2013).
7. Osterkamp, T. E. Characteristics of the recent warming of permafrost in Alaska. *J. Geophys. Res.* **112**, F02S02 (2007).
8. Elberling, B. *et al*. Long-term CO_2 production following permafrost thaw. *Nature Clim. Change* **3**, 890–894 (2013).
9. Brutsaert, W. & Hiyama, T. The determination of permafrost thawing trends from long-term streamflow measurements with an application in eastern Siberia. *J. Geophys. Res.* **117**, 1984–2012 (2012).
10. Kuhry, P. *et al*. Characterisation of the permafrost carbon pool. *Permafrost Periglac. Process.* **24**, 146–155 (2013).
11. Raich, J. W. & Schlesinger, W. H. The global carbon dioxide flux in soil respiration and its relationship to vegetation and climate. *Tellus B* **44**, 81–99 (1992).
12. Oberbauer, S. F. *et al*. Tundra CO_2 fluxes in response to experimental warming across latitudinal and moisture gradients. *Ecol. Monogr.* **77**, 221–238 (2007).
13. Hobbie, S. E. & Chapin, F. S. III The response of tundra plant biomass, aboveground production, nitrogen, and CO_2 flux to experimental warming. *Ecology* **79**, 1526–1544 (1998).
14. Dorrepaal, E. *et al*. Carbon respiration from subsurface peat accelerated by climate warming in the subarctic. *Nature* **460**, 616–619 (2009).
15. Natali, S. M., Schuur, E. A., Webb, E. E., Hicks Pries, C. E. & Crummer, K. G. Permafrost degradation stimulates carbon loss from experimentally warmed tundra. *Ecology* **95**, 602–608 (2014).
16. Sharp, E. D., Sullivan, P. F., Steltzer, H., Csank, A. Z. & Welker, J. M. Complex carbon cycle responses to multi-level warming and supplemental summer rain in the high Arctic. *Glob. Change Biol.* **19**, 1780–1792 (2013).
17. Lambers, H. III *et al*. *Plant Physiological Ecology* (Springer, 2008).
18. Davidson, E. A. & Janssens, I. A. Temperature sensitivity of soil carbon decomposition and feedbacks to climate change. *Nature* **440**, 165–173 (2006).
19. Dioumaeva, I. *et al*. Decomposition of peat from upland boreal forest: Temperature dependence and sources of respired carbon. *J. Geophys. Res.* **107**, 8222 (2002).
20. Hicks Pries, C. E., Schuur, E. A. G. & Crummer, K. G. Thawing permafrost increases old soil and autotrophic respiration in tundra: Partitioning ecosystem respiration using $\delta^{13}C$ and $\Delta^{14}C$. *Glob. Change Biol.* **19**, 649–661 (2013).
21. Schirrmeister, L. *et al*. Fossil organic matter characteristics in permafrost deposits of the northeast Siberian Arctic. *J. Geophys. Res.* **116**, 2005–2012 (2011).
22. Schuur, E. A. G. *et al*. The effect of permafrost thaw on old carbon release and net carbon exchange from tundra. *Nature* **459**, 556–559 (2009).
23. Ehleringer, J. R., Buchmann, N. & Flanagan, L. B. Carbon isotope ratios in belowground carbon cycle processes. *Ecol. Appl.* **10**, 412–422 (2000).
24. Trumbore, S. Age of soil organic matter and soil respiration: Radiocarbon constraints on belowground C dynamics. *Ecol. Appl.* **10**, 399–411 (2000).
25. Phillips, D. L. & Gregg, J. W. Source partitioning using stable isotopes: Coping with too many sources. *Oecologia* **136**, 261–269 (2003).
26. Bowling, D. R., McDowell, N. G., Bond, B. J., Law, B. E. & Ehleringer, J. R. ^{13}C content of ecosystem respiration is linked to precipitation and vapor pressure deficit. *Oecologia* **131**, 113–124 (2002).
27. Natali, S. M. *et al*. Effects of experimental warming of air, soil and permafrost on carbon balance in Alaskan tundra. *Glob. Change Biol.* **17**, 1394–1407 (2011).
28. Lupascu, M. *et al*. High Arctic wetting reduces permafrost carbon feedbacks to climate warming. *Nature Clim. Change* **4**, 51–55 (2014).
29. Nowinski, N. S., Taneva, L., Trumbore, S. E. & Welker, J. M. Decomposition of old organic matter as a result of deeper active layers in a snow depth manipulation experiment. *Oecologia* **163**, 785–792 (2010).
30. Hardie, S. M. L., Garnett, M. H., Fallick, A. E., Ostle, N. J. & Rowland, A. P. Bomb-^{14}C analysis of ecosystem respiration reveals that peatland vegetation facilitates release of old carbon. *Geoderma* **153**, 393–401 (2009).
31. Hicks Pries, C. E., Schuur, E. A. G., Vogel, J. G. & Natali, S. M. Moisture drives surface decomposition in thawing tundra. *J. Geophys. Res.* **118**, 1133–1143 (2013).
32. Natali, S. M., Schuur, E. A. & Rubin, R. L. Increased plant productivity in Alaskan tundra as a result of experimental warming of soil and permafrost. *J. Ecol.* **100**, 488–498 (2012).
33. Amthor, J. S. The McCree–de Wit–Penning de Vries–Thornley respiration paradigms: 30 years later. *Ann. Bot.* **86**, 1–20 (2000).
34. Shaver, G. R. *et al*. Biomass and CO_2 flux in wet sedge tundras: Responses to nutrients, temperature, and light. *Ecol. Monogr.* **68**, 75–97 (1998).
35. Rustad, L. *et al*. A meta-analysis of the response of soil respiration, net nitrogen mineralization, and aboveground plant growth to experimental ecosystem warming. *Oecologia* **126**, 543–562 (2001).
36. Keuper, F. *et al*. A frozen feast: Thawing permafrost increases plant-available nitrogen in subarctic peatlands. *Glob. Change Biol.* **18**, 1998–2007 (2012).
37. Blagodatskaya, E. & Kuzyakov, Y. Mechanisms of real and apparent priming effects and their dependence on soil microbial biomass and community structure: Critical review. *Biol. Fert. Soils* **45**, 115–131 (2008).
38. Hicks Pries, C. E. *et al*. Decadal warming causes a consistent and persistent shift from heterotrophic to autotrophic respiration in contrasting permafrost ecosystems. *Glob. Change Biol.* http://dx.doi.org/10.1111/gcb.13032 (2015).
39. Belshe, E. F., Schuur, E. A. G. & Bolker, B. M. Tundra ecosystems observed to be CO_2 sources due to differential amplification of the carbon cycle. *Ecol. Lett.* **16**, 1307–1315 (2013).
40. Grant, R. F., Humphreys, E. R., Lafleur, P. M. & Dimitrov, D. D. Ecological controls on net ecosystem productivity of a mesic arctic tundra under current and future climates. *J. Geophys. Res.* **116**, 2005–2012 (2011).

Acknowledgements

This work was made possible by assistance from J. Curtis, K. Venz-Curtis, A. B. Lopez, D. DeRaps, D. Rogan, E. Pegoraro and D. Hicks. This work was funded by NSF DDIG (C.E.H.P.), NSF CAREER (E.A.G.S.), Bonanza Creek LTER (E.A.G.S.), DOE NICCR and NSF OPP (S.M.N. and E.A.G.S.).

Author contributions

E.A.G.S. conceived and designed the warming experiment; S.M.N. designed and set up the warming experiment; C.E.H.P. designed the partitioning measurements, performed the field and lab work, analysed the data, and wrote the paper; K.G.C. performed lab analyses.

Additional information

Supplementary information is available in the online version of the paper. Reprints and permissions information is available online at www.nature.com/reprints. Correspondence and requests for materials should be addressed to C.E.H.P.

Competing financial interests

The authors declare no competing financial interests.

Methods

Site description. CiPEHR is located near Eight Mile Lake (EML, 63° 52′ 59″ N, 149° 13′ 32″ W) in Healy, Alaska. The vegetation consists of moist acidic tussock tundra dominated by *Eriophorum vaginatum* and includes the graminoid *Carex bigelowii*, dwarf shrubs *Vaccinium uliginosum*, *V. vitis-idaea*, *Betula nana*, *Rhododendron subarcticum*, *Rubus chamaemorus* and *Empetrum nigrum*, and various mosses and lichens[32]. The soils are histels and consist of 0.3–0.5 m of organic soil atop a mixture of mineral loess deposits and glacial till. Mean annual temperature is −2.3 °C and the active layer thaws to about 60 cm deep during the growing season[15]. Permafrost temperatures in the area are monitored via a borehole and have been increasing over the past several decades[7].

The soil warming (SW) and air warming (AW) treatments are set up in a factorial design: control, SW, AW and soil + air warming (SW + AW). In previous papers[15,27,32], soil warming was referred to as winter warming and air warming was referred to as summer warming. The air warming was achieved passively with open-top chambers (OTCs, 60 × 60 cm), and the soil warming was achieved with snowfences (8 m long by 1.5 m tall). The snowfences created snowdrifts over one metre deep, extending 10 m back from the fence that insulated soils throughout the winter[41]. At the end of each winter, excess snow was shovelled off the SW treatment so as not to add additional water or delay snowmelt. There were six replicate snowfences distributed evenly among three blocks. The SW treatment and SW control plots were the north and south sides of each fence, respectively. Each SW treatment and control plot contained both AW treatment and AW control plots.

Soil environment. In all plots, the soil temperature at three depths (5, 20, 40 cm) and the soil volumetric water content (VWC) averaged over the top 20 cm were recorded every half hour during the growing season[15]. Soil temperature was measured using constantan-copper thermocouples, and VWC was measured using site-calibrated Campbell CS616 water content reflectometer probes. Thaw depth (the depth from the soil surface to the frozen soil) was sampled at three points in each plot using a metal probe pushed into the soil until it hit frozen ground. Throughout the growing season, water table depth (WTD) was measured three times per week from water wells installed in each SW treatment and control plot (12 in total; ref. 15).

Ecosystem respiration. To measure the $\delta^{13}C$ and $\Delta^{14}C$ of R_{eco}, we installed 24 PVC collars (25.4 cm diameter × 10 cm deep) 6–7 cm into the soil, one per each of the four SW/AW treatment combinations at each of the six fences. We used previously published methods to sample $R_{eco}\delta^{13}C$ and $\Delta^{14}C$ (ref. 20). In brief, 10 l dark chambers were fitted onto the collars encompassing aboveground biomass. Ecosystem respiration $\delta^{13}C$ was analysed using the Keeling plot method, wherein CO_2 was collected into septa-capped glass vials (Exetainers, Labco Limited) every 2–3 min for a total of seven samples per collar, while an infrared gas analyzer (Licor-820, LICOR) simultaneously measured p_{CO_2}. The samples and a set of field standards (−10.46‰; Oztech Trading Corporation) with similar p_{CO_2} were sent back to the University of Florida to be run on a GasBench II coupled to a Finnigan Delta Plus XL stable isotope ratio mass spectrometer (precision ±0.2‰, $n=215$). $\delta^{13}C$ changes due to travel and holding time were corrected using the field standards. $R_{eco}\Delta^{14}C$ was collected by pumping CO_2 through a molecular sieve (Alltech 13x, Alltech Associates) for 15 min. Before the collection, the chamber headspace was scrubbed for 45 min with soda lime while maintaining ambient p_{CO_2} to remove atmospheric contamination. The molecular sieves were baked at 625 °C to desorb CO_2 (ref. 42), which was purified using liquid N_2 on a vacuum line and reduced to graphite by Fe reduction in H_2 (ref. 43). The graphite was sent to the UC Irvine W.M. Keck Carbon Cycle Accelerator Mass Spectrometry (AMS) Laboratory for radiocarbon analysis (precision ±2.3‰, $n=102$). $\Delta^{14}C$ data were reported at the same $\delta^{13}C$ value to correct for mass-dependent fractionation effects. $\Delta^{14}C$ data were corrected for atmospheric contamination using each chamber's $\delta^{13}C$ data in a two-pool (atmospheric and R_{eco}) mixing model[20]. R_{eco} isotopes were sampled at the beginning of July and in mid-September 2009, and in mid-August 2010 and 2011. Sampling occurred only under calm conditions and in the morning to control for potential diurnal variation. R_{eco} flux was measured from autochambers (60 × 60 cm each) adjacent to the PVC collars every 1.5 h throughout the growing season with a Licor-820 infrared gas analyzer (LICOR)[15,27].

Source respiration. Short-term incubations were used to measure the $\delta^{13}C$ and $\Delta^{14}C$ of autotrophic and heterotrophic source respiration[20]. We collected aboveground (AG) and belowground (BG) plant material to measure R_A isotopes by cutting 5 × 10 cm blocks of tundra down to the frozen soil from each treatment at each fence. Samples from the same treatment were combined by block, for a total of three AG and three BG replicates per treatment. We clipped all live AG plant material from each block and placed it in foil-covered Mason jars (0.24 l). Belowground roots and rhizomes (>1 mm diameter) were collected from the thawed soil, rinsed, and shaken dry before being put into their own Mason jars. We incubated plants as soon as possible after collection (within 5 min for AG and 30 for BG) to avoid changes to $\delta^{13}C$ that can occur 40 min to an hour after excision[44]. The jar headspace was scrubbed through soda lime for 5 min at >1 l min^{-1} before starting the incubations. $\delta^{13}C$ incubations lasted for 5–10 min, after which headspace air was pumped into He-flushed Exetainers. $\Delta^{14}C$ incubations lasted four hours, after which headspace CO_2 was collected into molecular sieves. Autotrophic respiration $\Delta^{14}C$ and $\delta^{13}C$ was measured at the beginning of July and in mid-September 2009, and in mid-August 2010 and 2011. Only SW treatment and control plots were sampled in July 2009 because the AW treatment had been ongoing only for six weeks, too soon to expect an AW treatment effect. Autotrophic respiration $\Delta^{14}C$ was sampled only from control plots in 2010 and 2011 because $R_A\Delta^{14}C$ did not differ significantly between SW and control plots in 2009 ($p=0.33$).

To measure the $\delta^{13}C$ and $\Delta^{14}C$ of heterotrophic respiration, we collected surface (0–25 cm) and deep (25–75 cm) soil cores. Surface soil cores were collected in SW treatment and control plots in July 2009 and from all treatments in August 2010. Because the isotopes of surface soil respiration did not change significantly from 2009 to 2010, we did not resample surface soils in August 2011. To core surface soils, we used a serrated knife to cut 5 × 5 cm blocks of soil, which were sectioned into 0–5 cm, 5–15 cm and 15–25 cm. As with the plant sampling, we combined samples from the same treatment within a block for a total of three replicates per treatment. We removed all roots >1 mm in diameter and let the surface soils sit at room temperature in Mason jars for five days before sampling $\delta^{13}C$ and $\Delta^{14}C$ to ensure sampling of the labile soil C pool and not recent root-derived C (ref. 20). Wait time was informed by a study wherein soil respiration rates decreased 50% five days after tree girdling[45] and from tundra soil incubations wherein the labile C pool was respired during the first 5–20 days[46,47]. In May 2009, we sampled deep soil cores (25–75 cm) while the ground was frozen using a Tanaka TIA-340 connected to a SIPRE coring auger. Cores were taken from the SW and control side of each fence for a total of 12 samples. Deep soil cores were kept frozen until we cut them into 10 cm sections, removed roots >1 mm diameter, and let them sit in Mason jars at room temperature for ten days to allow microbial populations to stabilize after thaw. For both shallow and deep soils, we measured R_H flux during three short (~3 h) incubations before sampling CO_2 for isotopic analysis. Soils were kept at field moisture and under aerobic conditions. For $\delta^{13}C$ and $\Delta^{14}C$ sample collection, we scrubbed CO_2 from the jar headspace, incubated the soils for 12–72 h (the time it took for 1.5 mg C to build up in the headspace), and pumped the headspace CO_2 into molecular sieves. The $\Delta^{14}C$ sample preparation and analysis was carried out as described for R_{eco}. However, after purification, a small (0.1–0.2 ml) subsample of CO_2 was removed and put in a He-filled Exetainer for $\delta^{13}C$ analysis. Source radiocarbon dates were converted to calendar dates using the Calib program[48].

Partitioning model. For partitioning R_{eco}, the R_H isotopes from the soil core depth sections were mathematically combined into two heterotrophic sources, young soil (YS, 0–15 cm) and old soil (OS, 15–75 cm) on the basis of the age of the respired CO_2. The YS source included soil sections that respired enriched 'bomb peak' $\Delta^{14}C$ from the past 50 years, and the OS included soil sections that respired older, depleted $\Delta^{14}C$ from the upswing of the bomb peak and earlier (Supplementary Table 6). To calculate $\delta^{13}C$ and $\Delta^{14}C$ values of YS and OS, we weighted the isotopic signatures of each incubated depth by its CO_2 flux per g soil, corrected for each depth sections' bulk density and average monthly field temperature (Supplementary Table 6; ref. 20). Each replicate core's weighted average was calculated, and then all cores were averaged to obtain mean $\delta^{13}C$ and $\Delta^{14}C$ for YS and OS. Before averaging, $\delta^{13}C$ values were corrected for a temperature shift[14,49], because incubation temperatures were warmer than field conditions. We used a Q_{10} of 2.5 and a $\delta^{13}C$ temperature correction of −0.16‰ per 1 °C (ref. 20) in the calculations described above. The same $\Delta^{14}C$ values from the 2009 deep soil cores (incubated in 2011) were used to calculate R_H sources for partitioning in all years, because changes in $\Delta^{14}C$ due to radioactive decay during that three-year time span were smaller than the 2.3‰ precision error of the AMS (ref. 22).

We used SIAR (Stable Isotope Analysis in R; ref. 50) to partition R_{eco} into two autotrophic (respiration of AG and BG plant material) and two heterotrophic sources (YS and OS). Partitioning was performed separately for each collar and sampling period. The SIAR method uses Markov chain Monte Carlo to find feasible solutions to this set of three equations:

$$^{13}C_{Ecosystem} = f_{AG}(^{13}C_{AG}) + f_{BG}(^{13}C_{BG}) + f_{YS}(^{13}C_{YS}) + f_{OS}(^{13}C_{OS})$$

$$^{14}C_{Ecosystem} = f_{AG}(^{14}C_{AG}) + f_{BG}(^{14}C_{BG}) + f_{YS}(^{14}C_{YS}) + f_{OS}(^{14}C_{OS})$$

$$1 = f_{AG} + f_{BG} + f_{YS} + f_{OS} \quad (1)$$

where the unknowns are f, each sources' proportional contribution to R_{eco}, and the $\delta^{13}C$ and $\Delta^{14}C$ of each source and R_{eco} have known distributions. The input data include the mean and standard deviation of all source isotopic values and the individual R_{eco} isotope values. An average AG and BG $R_A\delta^{13}C$ was used to partition all sampling periods and treatments, because there were no significant differences

within AG or BG $R_A\delta^{13}C$ among sampling periods or treatments. The July 2009 $R_A\Delta^{14}C$ values were used for September 2009 partitioning. The model output gives the probability density distributions of each sources' f. We used the default uninformative prior[50]. Previous sensitivity analyses found the results from this model to be robust to uncertainty in source parameters[20].

Data analysis. To investigate treatment and sampling date differences in the soil environment, isotopic values, and R_{eco} source contributions (mean f), we performed analyses of variance (ANOVAs) in JMP (SAS). The main effects were sampling date, the SW treatment, and the AW treatment nested within the SW treatment. For the soil environment variables, R_{eco} isotopes and source contributions, fence and plot nested within fence were the random effects. For source isotopes, block was a random effect (core was nested in block for soil isotopes), and type (AG/BG or YS/OS) was an additional main effect. For isotopes from individual soil sections, depth was an additional main effect. Source contributions were logit transformed before analyses. All residuals were checked for normality and homogeneity of variances to ensure ANOVA assumptions were met.

To explore how the soil environment affected $\Delta^{14}C$ and source contributions to R_{eco}, we performed multiple linear regressions in R (ref. 51). First, $\Delta^{14}C$ was square-root transformed, and source contributions were logit transformed to ensure normality. We included a depth-averaged soil temperature to 30 cm (ref. 52), VWC, WTD, thaw depth, and treatment as explanatory variables for $\Delta^{14}C$ and source contributions (Supplementary Tables 7 and 8). We used WTD measured 1–2 days before sampling and the thaw depth measured immediately after sampling. Other variables were measured continuously and were averaged over the sampling period. We used the full model to optimize random effects and variance structures using AIC values[53]. Random effects (block, fence, or plot) did not improve the AIC or explain variance, so they were not included. Visual checks, to make sure residuals did not vary with the random effects and that the residuals for each random effect were centred on zero, were performed to ensure independence was not violated. A power variance structure taking soil temperature and treatment into account improved the $\Delta^{14}C$ model, but not the source contribution models. Once random effects were optimized, we performed a series of pair-wise model comparisons using the F test: models were tested sequentially by dropping the least significant explanatory variable until only significant explanatory variables remained[53]. Ultimately, the $\Delta^{14}C$ model was fitted with the gls command in the nlme package[54] using restricted maximum likelihood, and the source contribution models were fitted with the base lm command.

We ran separate regressions to investigate how $R_{eco}\Delta^{14}C$ and OS proportional contributions were related to the average R_{eco} flux over each sampling period measured using autochambers (Supplementary Table 8; refs 15,27). To estimate the total amount C lost from old soil during the growing season, we related the OS proportional source contributions to R_{eco} flux and treatment. Unlike other regressions in this study, it was unclear whether treatment should be included in the model. Three models had AICc values within 4 units of one another. These included a model with just R_{eco} flux, one with R_{eco} flux and treatment, and one with R_{eco} flux, treatment and a flux by treatment interaction. We used AICc weights to average these three models using the AICcmodavg package in R (ref. 55). The average model was used to predict the proportion of R_{eco} coming from OS in each plot hourly throughout the growing season (1 May through 30 September). Because the model was fit to logit-transformed data, the predicted OS values had to be back transformed. To get the mean predicted values in the original unit of proportion, the variance had to be taken into account. The following equation was used to back transform:

$$\mu_{bt} = \frac{1}{(1+e^{\mu})^3}\left[e^{\mu}(1+e^{\mu}) + \frac{s^2}{2}e^{\mu}(1-e^{\mu})\right] \quad (2)$$

where μ is the mean predicted value from the model fit, s^2 is the variance, and μ_{bt} is the back-transformed predicted value. The OS proportion was then multiplied by the corresponding R_{eco} flux and summed over the growing season for each plot. This method was used to predict growing season losses of OS C for a −10 to −5 °C and −5 to 0 °C rise in MAT based on the R_{eco} and MAT relationship in a recent meta-analysis of tundra ecosystems[39].

References

41. Schuur, E. A. G. *et al*. Expert assessment of vulnerability of permafrost carbon to climate change. *Clim. Change* **119**, 359–374 (2013).
42. Bauer, J. E., Williams, P. M. & Druffel, E. R. Recovery of submilligram quantities of carbon dioxide from gas streams by molecular sieve for subsequent determination of isotopic carbon-13 and carbon-14 natural abundances. *Anal. Chem.* **64**, 824–827 (1992).
43. Vogel, J. S., Nelson, D. E. & Southon, J. R. ^{14}C background levels in an accelerator mass spectrometry system. *Radiocarbon* **29**, 323–333 (1987).
44. Midwood, A. J. *et al*. Collection and storage of CO_2 for ^{13}C analysis: An application to separate soil CO_2 efflux into root-and soil-derived components. *Rapid Commun. Mass Spectrom.* **20**, 3379–3384 (2006).
45. Högberg, P. *et al*. Large-scale forest girdling shows that current photosynthesis drives soil respiration. *Nature* **411**, 789–792 (2001).
46. Lavoie, M., Mack, M. C. & Schuur, E. a. G. Effects of elevated nitrogen and temperature on carbon and nitrogen dynamics in Alaskan arctic and boreal soils. *J. Geophys. Res.* **116**, G03013 (2011).
47. Lee, H., Schuur, E. A., Inglett, K. S., Lavoie, M. & Chanton, J. P. The rate of permafrost carbon release under aerobic and anaerobic conditions and its potential effects on climate. *Glob. Change Biol.* **18**, 515–527 (2012).
48. Stuiver, M., Reimer, P. & Reimer, R. *CALIB Radiocarbon Calibration* (2013); http://calib.qub.ac.uk/calib
49. Andrews, J. A., Matamala, R., Westover, K. M. & Schlesinger, W. H. Temperature effects on the diversity of soil heterotrophs and the $\delta^{13}C$ of soil-respired CO_2. *Soil Biol. Biochem.* **32**, 699–706 (2000).
50. Parnell, A. C., Inger, R., Bearhop, S. & Jackson, A. L. Source partitioning using stable isotopes: Coping with too much variation. *PLoS ONE* **5**, e9672 (2010).
51. R Development Core Team *R: A Language and Environment for Statistical Computing* (R Foundation for Statistical Computing, 2014); http://www.R-project.org
52. Risk, D., Kellman, L. & Beltrami, H. Carbon dioxide in soil profiles: Production and temperature dependence. *Geophys. Res. Lett.* **29**, 11-1–11-4 (2002).
53. Zuur, A. *et al*. *Mixed Effects Models and Extensions in Ecology with R* (Springer, 2009).
54. Pinheiro, J. *et al*. *nlme: Linear and Nonlinear Mixed Effects Models* (2013); http://CRAN.R-project.org/package=nlme
55. Mazerolle, M. *Model Selection and Multimodel Inference Based on (Q)AIC(c)* (2014); http://cran.r-project.org/web/packages/AICcmodavg/AICcmodavg.pdf